



## Characterisation of rheology and microstructures of $\kappa$ -carrageenan in ethanol-water mixtures

Zhi Yang<sup>a,b</sup>, Huijuan Yang<sup>a,c</sup>, Hongshun Yang<sup>a,b,\*</sup>

<sup>a</sup> Food Science and Technology Programme, c/o Department of Chemistry, National University of Singapore, Singapore 117543, Republic of Singapore

<sup>b</sup> National University of Singapore (Suzhou) Research Institute, 377 Lin Quan Street, Suzhou Industrial Park, Suzhou, Jiangsu 215123, PR China

<sup>c</sup> Synergetic Innovative Centre of Food Safety and Nutrition, Key Laboratory of Meat Processing and Quality Control, Ministry of Education, Key Laboratory of Animal Products Processing, Ministry of Agriculture, Jiangsu Innovative Centre of Meat Production and Processing, College of Food Science and Technology, Nanjing Agricultural University, Nanjing 210095, PR China



### ARTICLE INFO

#### Keywords:

Polysaccharide  
Sol-gel transition  
Rheology  
Solvent quality  
Network strength  
Small angle X-ray scattering

### ABSTRACT

The effects of ethanol (up to 20 wt%) on the rheological properties and structural characteristics of  $\kappa$ -carrageenan gel were investigated by Field Emission Scanning Electron Microscopy (FESEM) and Small Angle X-ray Scattering (SAXS). Both the sol-gel and gel-sol transition temperatures shifted to higher degree (from  $36.8 \pm 0.5$  to  $52.5 \pm 1.4$  °C and from  $51.2 \pm 0.6$  to  $67.0 \pm 0.5$  °C, respectively) upon 20 wt% ethanol addition ( $P < 0.05$ ). The critical relaxation exponent  $n$  and the critical gel strength  $S_g$  obtained from Winter-Chambon criterion decreased and increased, respectively as the ethanol concentration increased. The  $\kappa$ -carrageenan gel was formed due to the formation of fibrillar networks, and the fibrillar density increased upon ethanol addition via FESEM. Moreover, upon 20 wt% ethanol addition, the average radius of gyration of  $\kappa$ -carrageenan strand increased from  $1.18 \pm 0.03$  of control to  $1.55 \pm 0.02$  nm by SAXS. A mechanism underlying the effect of ethanol on the  $\kappa$ -carrageenan gelation was proposed based on coil to double helix transition followed by the helix aggregation.

### 1. Introduction

Kappa-carrageenan is a natural sulphated polysaccharide obtained from red seaweed predominately including *Chondrus*, *Gigartina*, and various *Eucheuma* species (Necas & Bartosikova, 2013). It has been traditionally used as thickener, stabilizer, and texturing agent in food, cosmetic, and pharmaceutical industries (Zhang et al., 2017). Recently,  $\kappa$ -carrageenan has been applied in bioactive encapsulation (Xu et al., 2014), wound healing (Aramwit, 2016), and multifunctional packaging (Rhim, 2013) due to its distinguished biocompatibility and biodegradability.

Kappa-carrageenan forms a thermoreversible gel in aqueous solution. It is generally considered that the gelation involves two steps: the initial random coil to helix transition and the aggregation of double helices upon introduction of mono or double positive ions such as  $K^+$ ,  $Na^+$ , and  $Ca^{2+}$  (Şen & Erboz, 2010). Many factors affect the sol-gel transition and the rheological and microstructural properties of the final gel. These factors include raw source from which  $\kappa$ -carrageenan was extracted (Yang et al., 2011), molecular weight (Leiter, Mailänder, Wefers, Bunzel, & Gaukel, 2017), introduction of ions (Robal et al.,

2017), and presence of sugar and polyols (Gekko, Mugishima, & Koga, 1987).

To date, most studies on  $\kappa$ -carrageenan gelation are in aqueous systems (Sow, Kong, & Yang, 2018). There are quite few investigations on the influence of mixed water and non-aqueous solvents (e.g. ethanol and methanol) on the rheological and microstructural properties of polysaccharide hydrogel, although this kind of study is pretty meaningful and important from both application and theoretical perspectives. For example, ethanol is usually employed in hydrogel based wound healing material primarily due to its antiseptic effect. The co-presence of  $\kappa$ -carrageenan and ethanol is not rare in food and beverage industries. Besides that, high concentrations of ethanol or methanol (usually higher than 50 wt%) are usually employed to decrease the solubility and precipitate  $\kappa$ -carrageenan from aqueous extracts. However, the effect of low concentration of ethanol (~20 wt%) on the sol-gel transition of  $\kappa$ -carrageenan remains unknown.

Introducing ethanol or methanol is an effective way to tune solvent quality of biopolymer aqueous system (Wang & Padua, 2010). The addition of ethanol up to 15% increased the mechanical strength of calcium alginate gels (Hermansson, Schuster, Lindgren, Altskär, &

\* Corresponding authors at: Food Science and Technology Programme, c/o Department of Chemistry, National University of Singapore, 3 Science Drive 3, Singapore 117543, Republic of Singapore.

E-mail address: [chmyngs@nus.edu.sg](mailto:chmyngs@nus.edu.sg) (H. Yang).

<https://doi.org/10.1016/j.foodres.2018.03.016>

Received 7 January 2018; Received in revised form 2 March 2018; Accepted 4 March 2018

Available online 07 March 2018

0963-9969/© 2018 Elsevier Ltd. All rights reserved.

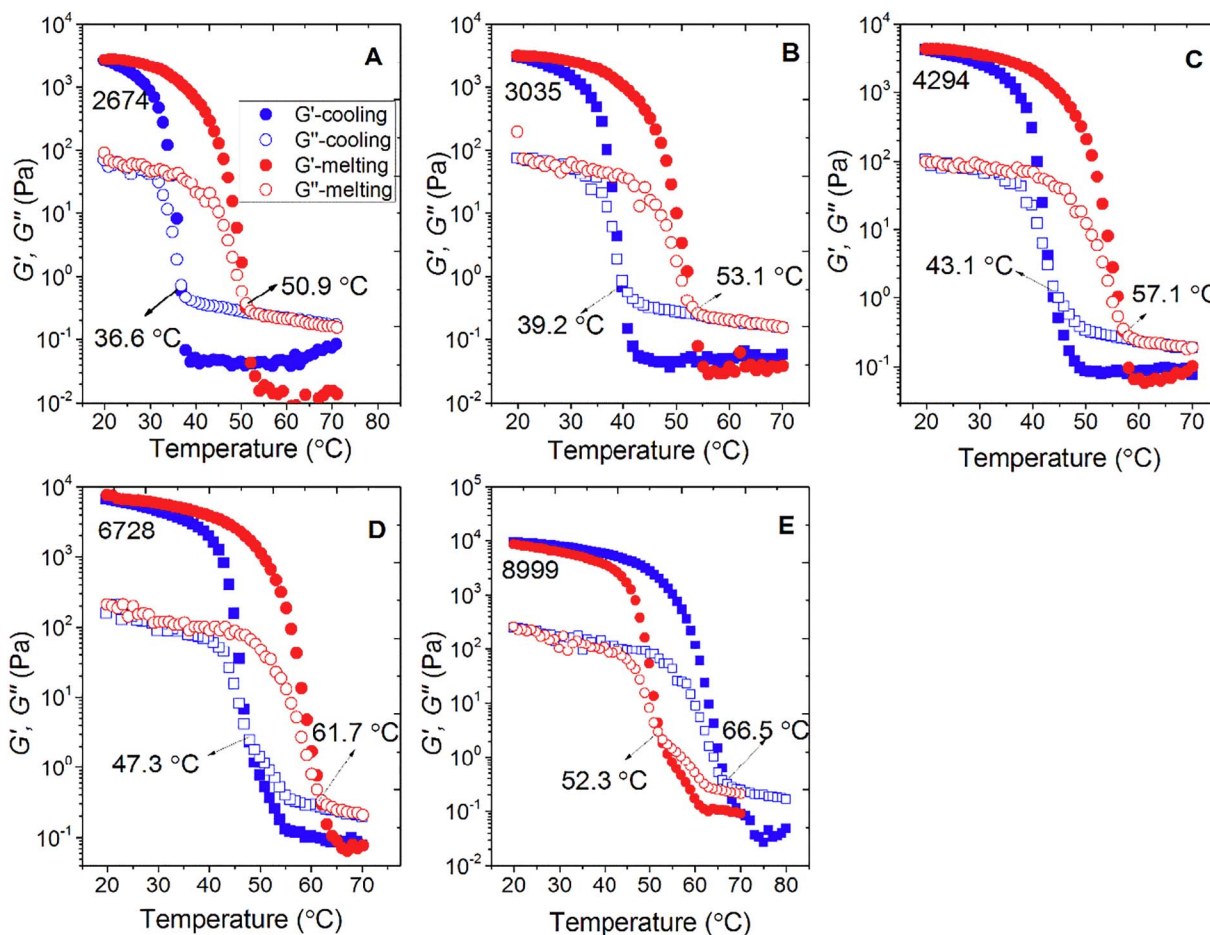


**Fig. 1.** Storage modulus ( $G'$ ) (solid symbols) and loss modulus ( $G''$ ) (open symbols) as a function of temperature during a rheological temperature sweep at the cooling and heating rate of 1  $^{\circ}\text{C}/\text{min}$  for 2 wt%  $\kappa$ -carrageenan solutions with addition of (A) 0 wt% ethanol, (B) 5 wt% ethanol, (C) 10 wt% ethanol, (D) 15 wt% ethanol, and (E) 20 wt% ethanol. All the standard deviation (SD) is < 7% of the mean value.

**Table 1**

Sol-gel transition ( $T_g$ ) and gel-sol transition ( $T_m$ ) temperature, thermal hysteresis ( $T_m - T_g$ ), storage modulus ( $G'$ ) (1 rad/s, 20  $^{\circ}\text{C}$ ), complex modulus ( $G^*$ ), and loss tangent  $\tan\delta$  (1 rad/s, 20  $^{\circ}\text{C}$ ) of  $\kappa$ -carrageenan with 0, 5, 10, 15, and 20 wt% ethanol additions. Codes typically as “KMS” are used. KM corresponds to  $\kappa$ -carrageenan. Numbers 0, 5, 10, 15, and 20 are corresponding to 0, 5, 10, 15, and 20 wt% ethanol additions, respectively.

Samples	$T_g$ ( $^{\circ}\text{C}$ )	$T_m$ ( $^{\circ}\text{C}$ )	$T_m - T_g$ ( $^{\circ}\text{C}$ )	$G'$ (Pa)	$G^*$ (Pa)	$\tan\delta \times 1000$
KM-0	$36.8 \pm 0.5^d$	$51.2 \pm 0.6^d$	$14.4 \pm 0.3^a$	$2620 \pm 127^d$	$3037 \pm 124^e$	$17.6 \pm 0.5^b$
KM-5	$39.6 \pm 0.4^d$	$53.5 \pm 0.7^d$	$13.9 \pm 0.4^a$	$2940 \pm 135^d$	$4850 \pm 332^d$	$20.7 \pm 1.3^{ab}$
KM-10	$43.4 \pm 0.8^c$	$57.6 \pm 0.8^c$	$14.2 \pm 0.5^a$	$4190 \pm 134^c$	$6254 \pm 220^c$	$20.3 \pm 1.1^{ab}$
KM-15	$47.7 \pm 0.8^b$	$62.3 \pm 0.6^b$	$14.6 \pm 0.6^a$	$6530 \pm 230^b$	$8448 \pm 353^b$	$23.4 \pm 1.2^a$
KM-20	$52.5 \pm 1.4^a$	$67.0 \pm 0.5^a$	$14.5 \pm 0.7^a$	$8920 \pm 150^a$	$13,138 \pm 430^a$	$24.4 \pm 0.7^a$

Values are demonstrated as mean  $\pm$  SD ( $n = 3$ ).

Different letters in the same column represent significant difference according to SPSS LSD test ( $P < 0.05$ ).

Ström, 2016). However, 20% ethanol reduced the gel strength and led to poorly and inhomogeneously connected network morphology. As a comparison, methanol (0–10%) impacted both the rheological properties and structural characteristics of pectin gel (Tho, Kjøniksen, Nyström, & Roots, 2003). Low concentration of methanol facilitated the gelation process and led to a strong gel while high concentration impeded gelation and caused a weak gel.

The gelation of  $\kappa$ -carrageenan in ethanol-water mixtures was chosen in the current study due to the versatile applications and precisely measurable dynamic modulus during the sol-gel and gel-sol transition. In addition, it allows us to study the effect of ethanol on the thermo-reversible gelation behaviour without adding any physical or chemical crosslinkers. The aim was to study the effect of ethanol addition on  $\kappa$ -carrageenan gel formation as well as gel melting. Although some

calorimetric studies related to  $\kappa$ -carrageenan in water-ethanol mixtures have been found in literature (Gekko et al., 1987), the effect of ethanol addition on its viscoelasticity and microstructure characteristics has not been reported. In this study, the Winter-Chambon criterion was employed to understand the sol-gel transition of  $\kappa$ -carrageenan as affected by ethanol addition. The Field Emission Scanning Electron Microscopy (FESEM) and Small Angle X-ray Scattering (SAXS) were used to characterise  $\kappa$ -carrageenan gel microstructure. The possible mechanism for sol-gel transition affected by ethanol was also proposed and discussed.

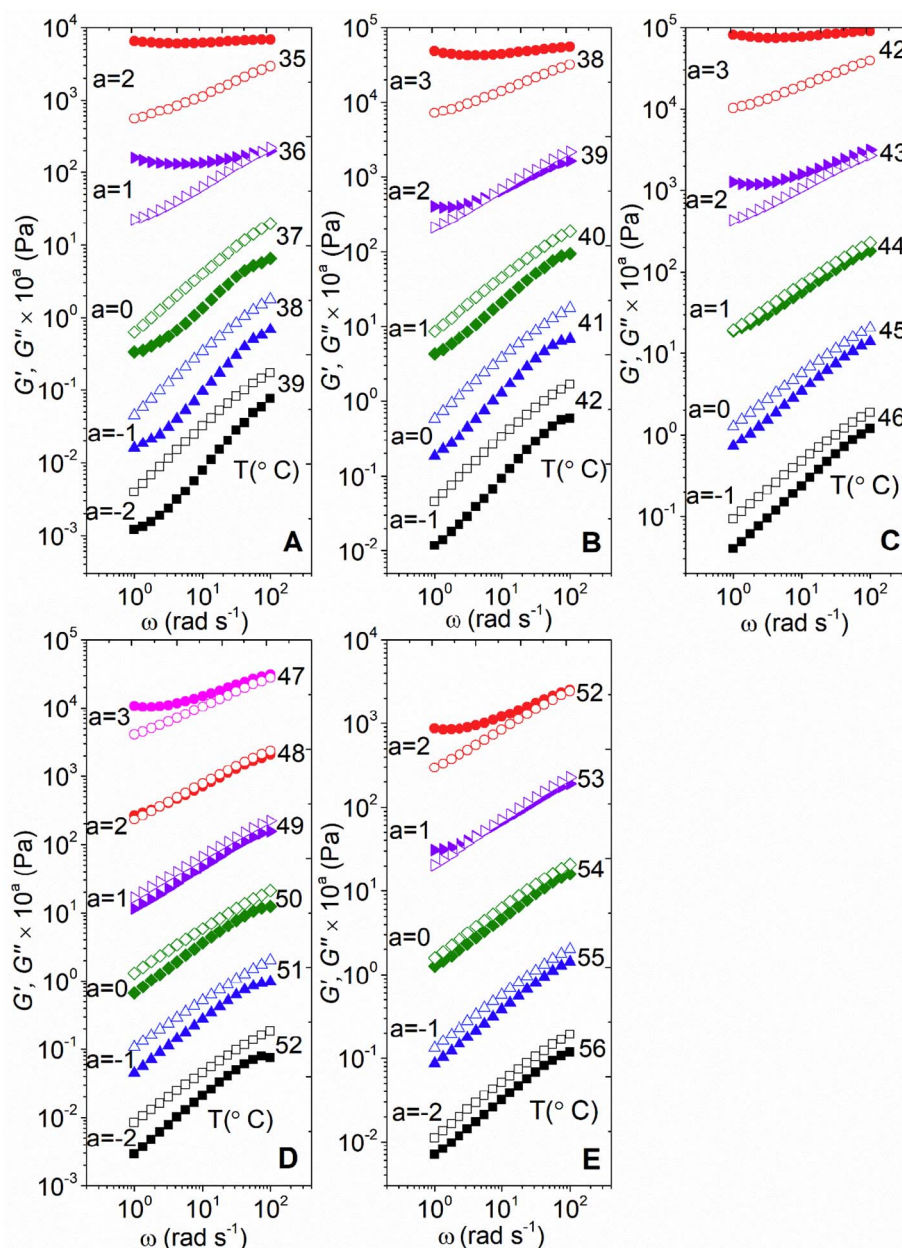


Fig. 2. Dependence of storage modulus  $G'$  (solid symbols) and loss modulus  $G''$  (open symbols), as a function of angular frequency  $\omega$  (rad/s) at different temperatures for 2 wt%  $\kappa$ -carrageenan solutions with addition of (A) 0 wt% ethanol, (B) 5 wt% ethanol, (C) 10 wt% ethanol, (D) 15 wt% ethanol, and (E) 20 wt% ethanol. To avoid overlapping, the data were shifted vertically by a factor of  $10^a$ . All the standard deviation (SD) is < 5% of the mean value.

## 2. Materials and methods

### 2.1. Materials

$\kappa$ -carrageenan powder (molecular weight of 300–400 kDa and composed  $\geq 93\%$  of  $\kappa$ -carrageenan as reported by the supplier) was obtained from Sigma Aldrich (Singapore). Ethanol (purity: 99.9 wt%) was obtained from Merck, USA. All raw materials were used without purification.

### 2.2. Sample preparation

A fixed mass of  $\kappa$ -carrageenan powder was dissolved respectively in ethanol-water containing 0, 5, 10, 15, and 20 wt% of ethanol under mild magnetic stirring at 80 °C in capped glass vials until the powder was fully swollen and solubilised to form homogeneous solution (Yang,

Yang, & Yang, 2018). The  $\kappa$ -carrageenan concentration in solution was constant, i.e. 2 wt%.

### 2.3. Rheological measurements

All the rheological measurements were conducted on a rotational stress controlled MCR 102 rheometer (Anton Paar GmbH, Graz, Austria) equipped with a stainless steel cone-and-plate geometry possessing a cone angle of 1° and diameter of 60 mm (truncated gap size: 210  $\mu$ m). The bottom plate was preheated to 80 °C before sample loading. A great care was taken to improve the reproducibility of the test and minimise the shear effect. For example, all the hot  $\kappa$ -carrageenan solutions were slowly poured into the bottom plate and relaxed for 10 min at 80 °C to destroy all the possible helical structures (Yang et al., 2018). To prevent water evaporation, a thin layer of sunflower oil was used to cover the free surface of samples. Strain sweep measurement in the range of

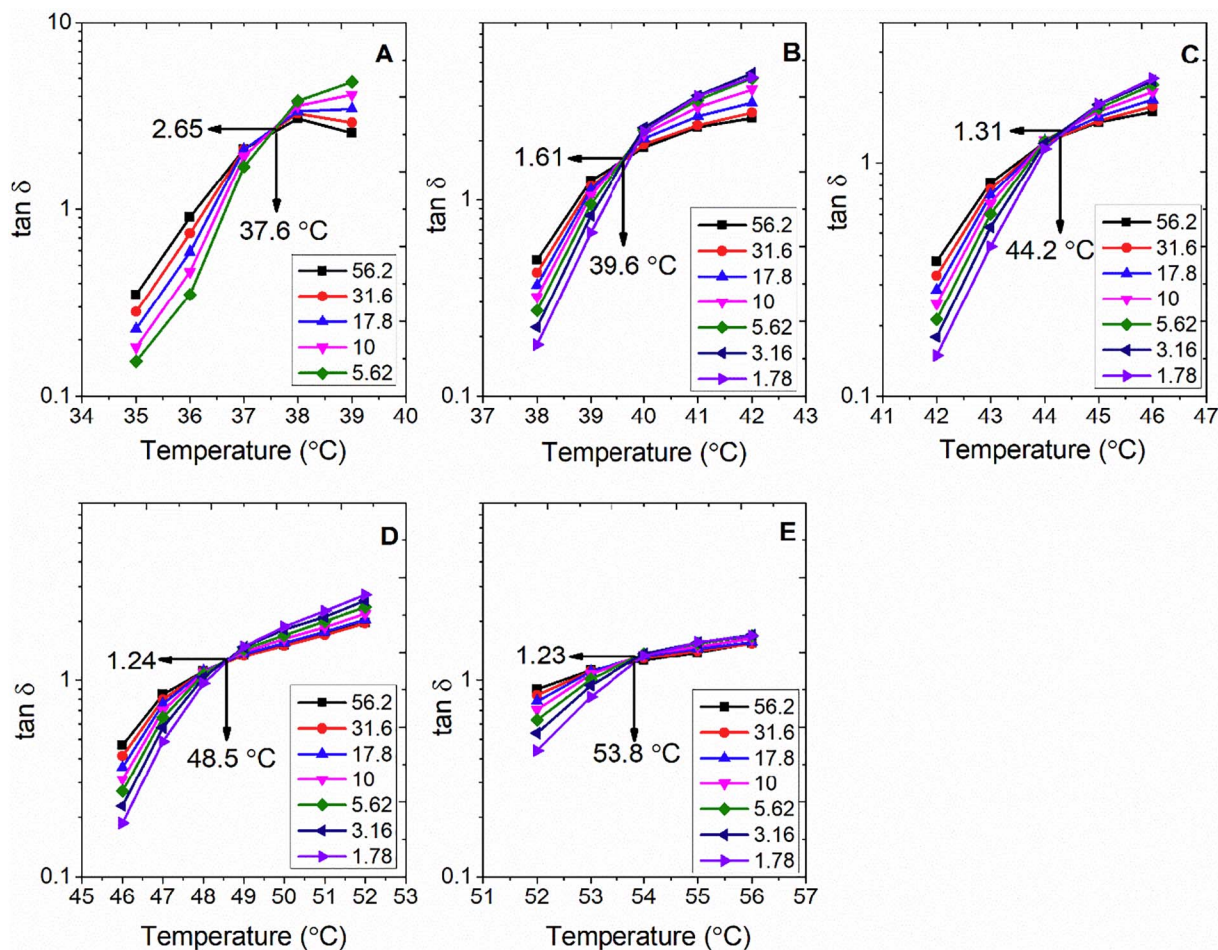


Fig. 3. Dependence of loss tangent,  $\tan\delta$ , as a function of temperature at different angular frequencies (rad/s) as depicted for 2 wt%  $\kappa$ -carrageenan solutions with addition of (A) 0 wt% ethanol, (B) 5 wt% ethanol, (C) 10 wt% ethanol, (D) 15 wt% ethanol, and (E) 20 wt% ethanol. All the standard deviation (SD) is < 5% of the mean value.

0.1–10,000% at angular frequency 1 rad/s was performed to determine the Linear Viscoelastic Region (LVR) of the samples in both solution and gel states. The following three rheological characterisation protocols were applied to examine the rheological evolution of  $\kappa$ -carrageenan solutions. Each measurement was repeated in triplicate.

2.3.1. Temperature sweep

To study the changes in viscoelasticity as a function of temperature, the samples were subject to a temperature sweep from 80 to 20 °C, held at 20 °C for 5 min, and then heated up to 80 °C (Nieto, Wang, Ozimek, & Chen, 2016). The gelation and melting temperature was defined as the temperature where  $G' = G''$  or  $\tan \delta (G'' / G') = 1$  (Li et al., 2018). The cooling and heating rate was set at 1 °C/min with a fixed strain of 1% and angular frequency of 1 rad/s.

2.3.2. Frequency sweep test

The frequency sweep (100–1 rad/s) was conducted at various temperatures near sol-gel transition temperature obtained in protocol 2.3.1 at a constant strain of 1% within Linear Viscoelastic Region (LVR) relating to the ethanol concentration.

As described in the Section 2.3.1, the gel point can be identified by the temperature at the crossover of storage modulus  $G'$  and loss modulus  $G''$  using temperature sweep measurement. However, the gel temperature determined using this protocol is strongly dependent on the frequency and cooling rate employed (Liu, Li, Tang, Bi, & Li, 2016). The more accurate way to resolve the frequency independent gel temperature was proposed by Winter's and his colleagues that at the gelling point, both  $G'$  and  $G''$  demonstrate the power-law dependence of

frequency (Chambon & Winter, 1985, 1987):

$$G'(\omega) \sim G''(\omega) \sim \omega^n \tag{1}$$

and

$$\tan \delta = \frac{G''(\omega)}{G'(\omega)} = \tan\left(\frac{n\pi}{2}\right) \tag{2}$$

where  $\tan\delta$  and  $n$  are the loss factor and critical relaxation exponent, respectively. The gel point also named as “Winter-Chambon criterion” was determined at which the loss factor was independent of frequency (Tho et al., 2003).

The critical relaxation exponent  $n$  depends on its relationship with fractal dimension  $d_f$ . Assuming that the variation of the excluded volume effect is induced by the change of strand length between cross-linking points, Muthukumar (1989) developed a theoretical model to describe the relationship between  $n$  and fractal dimension  $d_f$ :

$$n = \frac{d(d + 2 - 2d_f)}{2(d + 2 - d_f)} \tag{3}$$

where  $d$  ( $d = 3$ ) is the space dimension and  $d_f$  is the fractal dimension.

Apart from  $n$  and  $d_f$ , another important parameter to depict the critical gel property is the critical gel strength  $S_g$ , which was derived from the power law behaviour of the shear relaxation modulus  $G(t)$  at the critical gelation point:

$$G(t) = S_g t^{-n} \tag{4}$$

The physical meaning of  $S_g$  is the relaxation modulus at the gel point when the relaxation time  $t$  equals 1 s and relates to the gel strength at

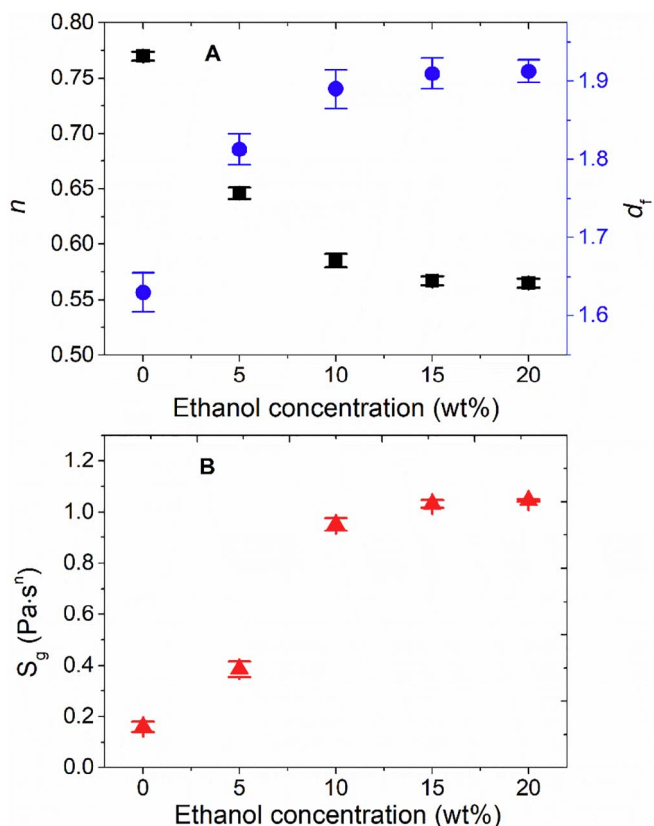


Fig. 4. Dependence of (A) the critical relaxation exponent  $n$  (square) and fractal dimension  $d_f$  (sphere) and (B) the critical gel strength  $S_g$  with ethanol concentration.

gel point.  $S_g$  can be calculated from the following equation when  $G'$  or  $G''$  is known at the gel point:

$$G'(\omega) = G''(\omega) / \tan\left(\frac{n\pi}{2}\right) = S_g \omega^n \Gamma(1 - n) \cos\left(\frac{n\pi}{2}\right) \quad (5)$$

where  $\Gamma(1 - n)$  is the Gamma function.

Furthermore, the complex modulus  $G^*$  can be obtained by.

$$G^* = (G'^2 + G''^2)^{0.5} \quad (6)$$

### 2.3.3. Small deformation oscillatory shear rheology

Frequency sweep was employed to evaluate the small deformation

viscoelasticity of  $\kappa$ -carrageenan/water/ethanol system below its sol-gel transition point at 20 °C. To initiate gel formation, the temperature was declined from 80 to 20 °C at 1 °C/min. During gelation, time sweep measurement was conducted at a constant angular frequency 1 rad/s with a constant strain 1% to examine gelation evolution for 5 h. After that, the frequency sweep measurement was performed and  $G'$  and  $G''$  were measured as a function of angular frequency from 100 to 0.1 rad/s at 20 °C. The complex modulus was calculated by the Eq. (6). All rheological measurements were performed within a predetermined Linear Viscoelastic Region (LVR) through preliminary strain sweep measurement with fixed strain amplitude at 1% (Yang et al., 2015).

### 2.4. SAXS

Synchrotron SAXS measurements were carried out on the beamline BL16B1 at the Shanghai Synchrotron Radiation Facility (SSFR, Shanghai, China) at room temperature (~25 °C). The  $\kappa$ -carrageenan solutions were transferred in a multiple position sample holder sealed with Kapton tapes on both sides, and left for 12 h at 20 °C to ensure that the gel was fully developed before SAXS measurement. All the data collected were background subtracted from the scattering of Kapton tapes and solvents and processed using FIT2D software (<http://www.esrf.eu/computing/scientific/FIT2D/>).

Symbols  $q$  and  $I(q)$  stand for the scattering vector and scattering intensity (unit is a.u.), respectively. The sample-to-detector distance was set such that the detecting range  $q$  was between 0.8 and 1.8 nm<sup>-1</sup> and  $q = \frac{4\pi \sin \theta}{\lambda}$  (where  $2\theta$  is the scattering angle and  $\lambda = 1.24 \text{ \AA}$  is the X-ray wavelength). The cross-sectional radius ( $R_c$ ) was calculated based on previous reports on the condition that  $q_{\max} R_c < 1$  (Stokke et al., 2000; Yang et al., 2018).

### 2.5. FESEM

The microstructures of  $\kappa$ -carrageenan/water/ethanol hydrogels were characterized using a FESEM (JSM-6701F, JEOL, Japan) with accelerating voltage 5 kV. The hydrogel samples were freeze dried at -80 °C for 5 days and sputtered with platinum on the surface under vacuum before FESEM characterisation. Each sample was prepared in duplicate and at least three representative areas from the same sample were examined.

### 2.6. Statistical analyses

All the experiments were performed in triplicate and the results

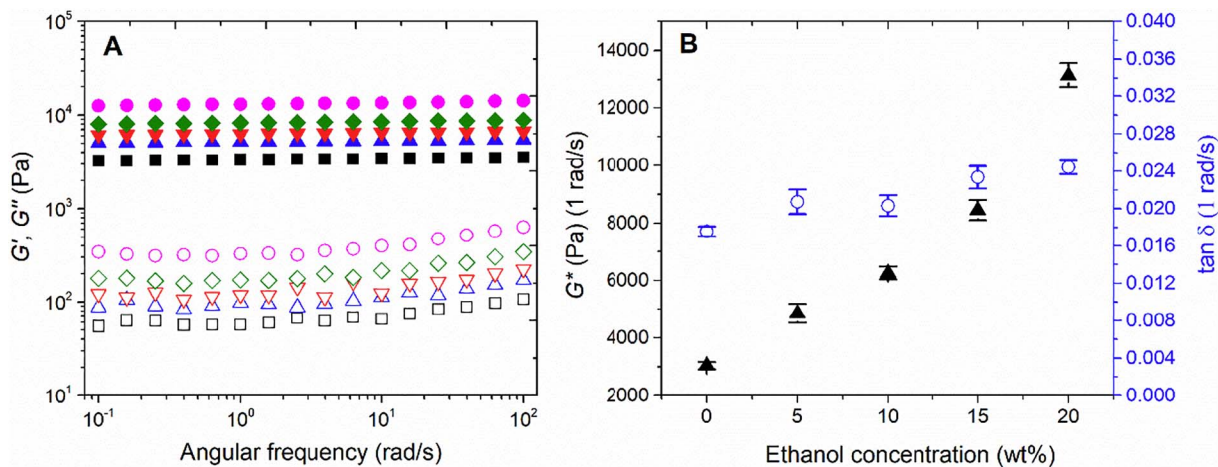


Fig. 5. (A) Dynamic viscoelastic storage modulus  $G'$  (solid symbols) and loss modulus  $G''$  (open symbols) as a function of frequency for  $\kappa$ -carrageenan gel with various amounts of ethanol additions, (B) The complex modulus  $G^*$  (triangle) and  $\tan \delta$  (circle) at 1 rad/s as a function of ethanol addition. Ethanol concentrations are: 0% (■, □); 5% (▲, △); 10% (▼, ▽); 15% (◆, ◇); 20% (●, ○). All measurements were taken at 20 °C. All the standard deviation (SD) is < 8% of the mean value.

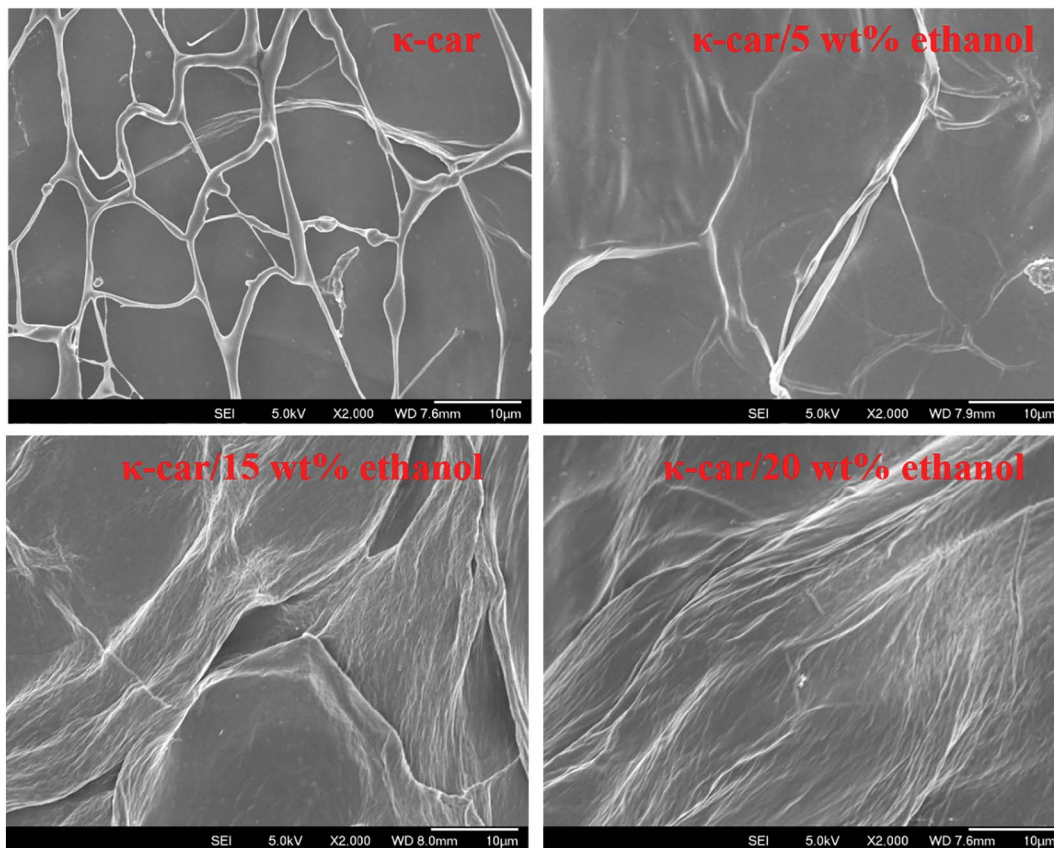


Fig. 6. FESEM images of 2 wt%  $\kappa$ -carrageenan hydrogels with various amounts of ethanol additions. Gels were freeze-dried prior to analysis.

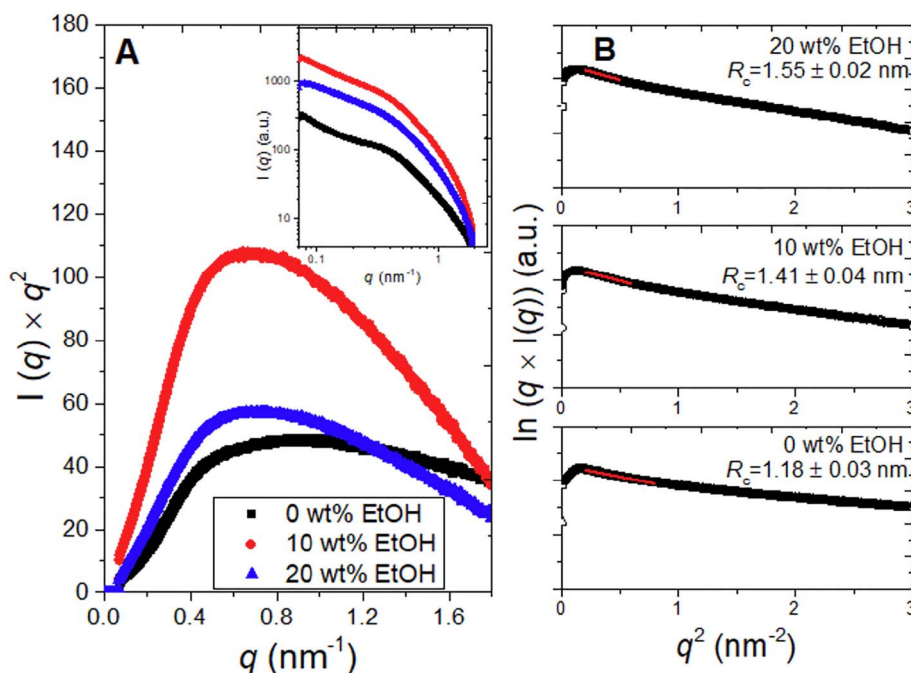


Fig. 7. (A) Kratky plots of the SAXS scattering profiles of 2 wt%  $\kappa$ -carrageenan solutions with various amounts of ethanol additions and the SAXS profiles  $I(q)$  (insert). (B) Cross-sectional Guinier plots of the SAXS profiles. The red solid line indicates the Guinier region. (For interpretation of the references to colour in this figure legend, the reader is referred to the web version of this article.)

were expressed as mean  $\pm$  standard deviation (SD). Analysis of variance (ANOVA) using the Least Significant Difference (LSD) test for mean comparisons was performed using the SPSS package 21.0 (Chicago, IL, USA). The significance was set at  $P < 0.05$ .

### 3. Results

#### 3.1. Thermoreversible behaviour of various $\kappa$ -carrageenan hydrogels

The influence of temperature on the sol-gel and gel-sol transitions of  $\kappa$ -carrageenan hydrogels containing various amounts of ethanol is shown in Fig. 1. At high temperatures,  $G''$  was greater than  $G'$ . Upon

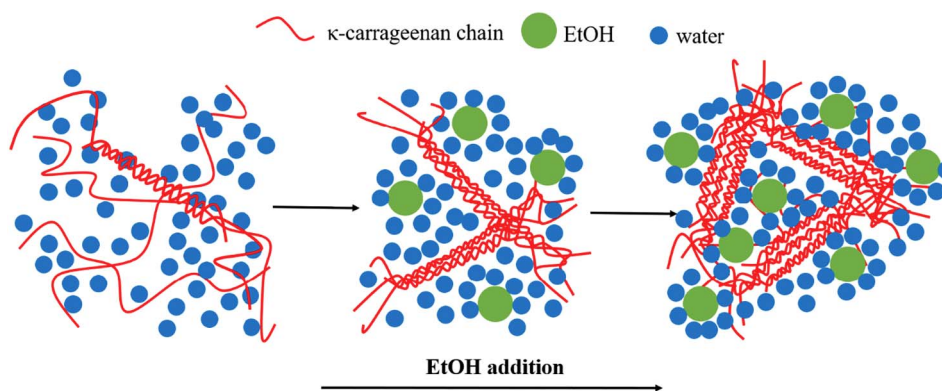


Fig. 8. A schematic illustration of the sol-gel transition of  $\kappa$ -carrageenan hydrogels as affected by ethanol addition.

cooling, both  $G'$  and  $G''$  increased marginally. However, with continued cooling,  $G'$  increased significantly faster than  $G''$  and at certain point, crossover of  $G'$  and  $G''$  occurred. The crossover at  $36.8 \pm 0.5^\circ\text{C}$ ,  $39.6 \pm 0.4^\circ\text{C}$ ,  $43.4 \pm 0.8^\circ\text{C}$ ,  $47.7 \pm 0.8^\circ\text{C}$ ,  $52.5 \pm 1.4^\circ\text{C}$  was identified as sol-gel transition temperature ( $T_g$ ) for  $\kappa$ -carrageenan containing 0, 5, 10, 15, and 20 wt% ethanol, respectively (Table 1). In general,  $T_g$  increased as ethanol concentration increased ( $P < 0.05$ ) although there was no significant difference between sole  $\kappa$ -carrageenan samples and that containing 5 wt% ethanol ( $P > 0.05$ ). The  $G'$  values at the lowest temperature  $20^\circ\text{C}$  increased from  $2620 \pm 127$  to  $8920 \pm 150$  Pa when ethanol concentration increased to 20 wt% ( $P < 0.05$ ) (Table 1).

In the subsequent heating process, the gel network was destroyed as demonstrated by the reduction of both  $G'$  and  $G''$ . The reduction rate of  $G'$  with temperature was faster than that of  $G''$ . Thus, crossover of  $G'$  and  $G''$  occurred again where the temperature was defined as the critical temperature and considered as the gel-sol transition or melting temperature ( $T_m$ ). The  $T_m$  increased from  $51.2 \pm 0.6^\circ\text{C}$  to  $67.0 \pm 0.5^\circ\text{C}$  with ethanol increased to 20 wt% ( $P < 0.05$ ) (Table 1), although 5 wt% of ethanol had no significant impact on  $T_m$  ( $P > 0.05$ ). If the temperature difference between  $T_g$  and  $T_m$  was defined as thermal hysteresis  $\Delta T$ ,  $\Delta T$  was determined to be  $14.4 \pm 0.3^\circ\text{C}$ ,  $13.9 \pm 0.4^\circ\text{C}$ ,  $14.2 \pm 0.5^\circ\text{C}$ ,  $14.6 \pm 0.6^\circ\text{C}$ , and  $14.5 \pm 0.7^\circ\text{C}$  for  $\kappa$ -carrageenan containing 0, 5, 10, 15, and 20 wt% ethanol, respectively (Table 1). Apparently, ethanol addition had no significant impact on  $\Delta T$  ( $P > 0.05$ ).

### 3.2. Critical viscoelastic behaviour of various $\kappa$ -carrageenan hydrogels at sol-gel transition

Fig. 2 illustrates  $G'$  and  $G''$  as a function of frequency at various temperatures near sol-gel transition temperature, showing how  $\kappa$ -carrageenan solutions transitioned from liquid to solid-like gels. At high temperature such as  $39^\circ\text{C}$ ,  $G''$  dominated over  $G'$  within the full angular frequency range. When the temperature was decreased, e.g. around  $38^\circ\text{C}$ ,  $G'$  and  $G''$  were nearly parallel with each other and exhibited a similar power law dependence with frequency. With further temperature decrease to  $36^\circ\text{C}$ ,  $G'$  began to crossover with  $G''$  and finally  $G'$  dominated over  $G''$  in the entire frequency range. Overall, the  $\kappa$ -carrageenan containing different amounts of ethanol showed a similar behaviour.

In order to apply the Winter-Chambon criterion to determine the critical gelation temperature, the critical loss factor  $\tan \delta$  was plotted versus the gelling variable, at various angular frequencies (Fig. 3). The gel points were determined from the frequency-independent points of these multi-frequency plots. For all the samples, the multifrequency curves crossed at certain temperatures, which were defined as the critical gelation temperature and which were  $37.6 \pm 0.3^\circ\text{C}$ ,  $39.4 \pm 0.5^\circ\text{C}$ ,  $43.8 \pm 0.5^\circ\text{C}$ ,  $48.0 \pm 0.6^\circ\text{C}$ , and  $53.2 \pm 0.7^\circ\text{C}$  for

the  $\kappa$ -carrageenan gels containing 0, 5, 10, 15, and 20 wt% ethanol, respectively. With the known critical gelation temperature, the critical loss factor that corresponds to it was identified (Fig. 3). With ethanol increased from 0 to 20 wt%, the critical relaxation exponent  $n$  decreased from  $0.76 \pm 0.05$  to  $0.56 \pm 0.03$  ( $P < 0.05$ ) (Fig. 4A). However, the fractal dimension  $d_f$  increased from  $1.63 \pm 0.04$  to  $1.91 \pm 0.02$ , and  $S_g$  increased from  $0.16 \pm 0.02$  to  $1.04 \pm 0.01$  Pa with ethanol concentration increased to 20 wt% ( $P < 0.05$ ) (Fig. 4).

### 3.3. Small deformation viscoelasticity of various $\kappa$ -carrageenan hydrogels

The  $\kappa$ -carrageenan gels with various amounts of ethanol did not reach equilibrium, showing a continuously increasing  $G'$  over 5 h (Fig. S1). However, at long gelation time, i.e., 5 h, the gelation kinetics remained at a low level, becoming appropriate for frequency sweep measurement.

The  $G'$  and  $G''$  as a function of frequency for various  $\kappa$ -carrageenan hydrogels is demonstrated in Fig. 5A. For all the samples,  $G'$  dominated over  $G''$  by approximately 100 times in the full frequency range. In addition, both  $G'$  and  $G''$  were nearly independent of frequency in the range between 100 and 0.1 rad/s. Moreover,  $G'$  and  $G''$  increased with increased amount of ethanol. The complex modulus  $G^*$  which took into consideration of both  $G'$  and  $G''$  increased nearly linearly with the addition of ethanol up to 20 wt% ( $P < 0.05$ ) (Fig. 5B), indicating a strengthening effect of ethanol on the  $\kappa$ -carrageenan hydrogel network. Among all the ethanol concentrations, the value of  $\tan \delta$  at 1 rad/s was much smaller than 0.1 and increased slightly from 0.018 to 0.024 at 20 wt% of ethanol (Fig. 5B and Table 1).

### 3.4. FESEM characterisation

The microstructures of  $\kappa$ -carrageenan gels with various amounts of ethanol after freeze drying are illustrated in Fig. 6. At 5 wt% ethanol, the overall microstructures of the  $\kappa$ -carrageenan hydrogel didn't change as compared to sole  $\kappa$ -carrageenan hydrogel. It showed interconnected, porous, cell wall-like structures with relatively large open area (voids) in between, characteristic of  $\kappa$ -carrageenan gels. However, the gel morphology changed as the ethanol concentration increased from 5 wt% to 20 wt%. With 15 wt% and 20 wt% ethanol, finely and densely packed  $\kappa$ -carrageenan strands closely resembled in the gel matrices were observed.

### 3.5. SAXS analysis

Fig. 7A shows the Kratky plots of  $\kappa$ -carrageenan gels and their corresponding SAXS patterns. A peak was observed in the Kratky plots, which shifted to lower  $q$  as ethanol concentration increased. To quantify the junction zone dimensions induced by network aggregation, cross-sectional Guinier plots ( $\ln(qI(q))$  vs.  $q^2$ ) were employed to obtain

cross-sectional radius ( $R_c$ ) of  $\kappa$ -carrageenan chains (Fig. 7B). Given that the  $\kappa$ -carrageenan molecule had a rigid cylinder structure, of which the  $R_c$  was much smaller than the length, as revealed by X-ray diffraction studies. As a result,  $R_c$  was  $1.18 \pm 0.03$  nm (0 wt% ethanol),  $1.41 \pm 0.04$  nm (10 wt% ethanol), and  $1.55 \pm 0.02$  nm (20 wt% ethanol).

#### 4. Discussion

The gel points can be determined from the frequency-independent points of multi-frequency plots (Liu, Bao, & Li, 2016; Wu, Cui, Eskin, & Goff, 2009). When increased temperature to a certain level,  $G''$  exceeded  $G'$  demonstrating that the system was transformed into viscoelastic liquid (Lu, Liu, Dai, & Tong, 2005), which might be attributed to the loss of double helical structures (Zhu et al., 2008). Vice versa, when decreased to 36 °C,  $G'$  began to crossover with  $G''$  and finally  $G'$  turned to dominate over  $G''$  (Cuvelier & Launay, 1990).

From the temperature sweep measurement,  $T_g$ ,  $T_m$  and  $G'$  (1 rad/s) at 20 °C increased considerably with increased ethanol concentration (Fig. 1 and Table 1), which is consistent with previous report (Gekko et al., 1987). The presence of ethanol (> 5 wt%) might increase the stability of the gel networks which required more thermal energy to deteriorate, leading to increased  $T_m$  (Liu, Huang, & Li, 2016). For all the  $\kappa$ -carrageenan gels,  $T_g$  was lower than  $T_m$ , which is the origin of the hysteresis behaviour during coil-helix and helix-coil transition loops. The transition from coils to helices is more energetically feasible and occurs at lower temperature; however, the dissociation of helices to coils needs more energy, thus requiring higher temperature (Tari, Kara, & Pekcan, 2009).

The critical gelation temperature obtained by the Winter-Chamber criterion agreed well with the  $T_g$  obtained from crossover of  $G'$  and  $G''$ . Similar result has been found in  $\kappa$ -carrageenan/ $\text{Ca}^{2+}$  systems (Liu & Li, 2016). Meanwhile, the relaxation exponent  $n$  changes from 0 to 1 along with the phase angle  $\delta$  varying from  $\pi/2$  to 0. More specifically,  $n = 1$  suggests a fully viscous liquid while  $n = 0$  indicates a completely elastic solid. Therefore, the decrease of  $n$  with increased ethanol suggested that the sol-gel transition occurred near elastic solid or far from viscous liquid. These findings agree well with previous reports including pectin/methanol (Tho, Kjøniksen, Knudsen, & Nyström, 2006) and alginate/ $\text{Ca}^{2+}$  (Liu & Li, 2016). The enhanced gel strength of gels containing added chemicals such as methanol was ascribed to the favourable formation of intermolecular associations and hydrogen-bonded complexes between the gel reagent and the added chemical (Tho et al., 2006).

In the current study, the structure of  $\kappa$ -carrageenan gels containing ethanol was revealed by the frame work of fractal dimension  $d_f$  and critical gel strength  $S_g$ . The greater value of  $d_f$ , the compacter and denser structures that materials possess (Beaucage, 1996). Therefore, the greater  $d_f$  observed in  $\kappa$ -carrageenan containing larger amount of ethanol suggested that ethanol strengthened  $\kappa$ -carrageenan gel network. This result is similar as previous report about pectin added with methanol (Tho et al., 2006). In terms of  $S_g$ , it has been suggested that it is related to the amount and/or size of gel network junctions (Liu & Li, 2016). Thus, the increased  $S_g$  by ethanol indicated more gel network junctions were formed in  $\kappa$ -carrageenan gel added with ethanol than sole  $\kappa$ -carrageenan gel, which contributed to a greater gel strength. This result agrees with the previously reported  $\kappa$ -carrageenan hydrogel/ $\text{Ca}^{2+}$  system (Liu & Li, 2016).

The strengthening effect of ethanol on  $\kappa$ -carrageenan gel was also confirmed by small oscillatory deformation study (Fig. 5A), which showed  $G^*$  increased with increased amount of ethanol. Moreover, all the  $\tan \delta$  values were smaller than 0.1, indicating that all the  $\kappa$ -carrageenan gels contained a strong gel network (Lapasin, 1995). The slight increase of  $\tan \delta$  by increased amount of ethanol suggested that ethanol slightly facilitated the conversion of  $G''$  to  $G^*$ . However, the mechanism underlying the slight increase of  $\tan \delta$  induced by ethanol is still not clear and needs further study.

The rheological results suggested that ethanol addition promoted the sol-gel transition and further aggregated  $\kappa$ -carrageenan helices, thereby promoting the gel network strength. The similar phenomenon was also found in alginate gel/ $\text{Ca}^{2+}$  aqueous solution added with ethanol (Hermansson et al., 2016) and pectin gel added with methanol (Tho et al., 2003).

The microstructure of  $\kappa$ -carrageenan gels via FESEM was consistent with their rheological properties. This structure relates to the mechanical strength of gel (Hu, Lu, Zhao, & Matsukawa, 2017; Miyabe et al., 2017). For  $\kappa$ -carrageenan hydrogel without containing ethanol, an interconnected, porous, cell wall-like structure formed, which is characteristic of  $\kappa$ -carrageenan gels and might be formed during freeze drying (Denef, Mischenko, Koch, & Reynaers, 1996; Hilliou, Wilhelm, Yamanoi, & Gonçalves, 2009; Lorén et al., 2009). The gel network can be facilitated by elongation and rearrangement of the polymer chain (Joly-Duhamel, Hellio, Ajdari, & Djabourov, 2002). Typical characteristic of strong gel networks shows solid-like behaviour (Kavanagh & Ross-Murphy, 1998; Yang et al., 2016).

The denser and compacter fibrillar structures in  $\kappa$ -carrageenan gels containing 15 wt% and 20 wt% ethanol correlated well with their greater  $d_f$  values. SAXS exhibits a great advantage on determining the nanostructures of hydrogels in their natural state so that the complications of sample preparation procedures such as drying and oxidative dyeing are avoided (Hollamby, 2013).

The peak shown in the recorded  $q$ -range in all the Kratky plots suggested a three-dimensional mass fractal system composing of molecular aggregates was developed in all the  $\kappa$ -carrageenan gels (Hermansson et al., 2016; Hirun, Tantishaiyakul, Sangfai, Rugmai, & Soontaranon, 2016). The similar Kratky plots of hydrogels induced by molecular structure aggregation and interconnection have also been reported in other biopolymer hydrogels such as  $\text{Ca}^{2+}$ -Alginate gel (Stokke et al., 2000) and pectin gel (Schuster, Cucheval, Lundin, & Williams, 2011). Upon increasing ethanol addition, the peak of the Kratky plot was shifted to smaller  $q$ -values. This together with the cross-sectional Guinier analysis implied the formation of junctions of greater size and cross-sectional radii, a result caused by helices association and aggregation (Teodorescu, Morariu, Bercea, & Sacarescu, 2016).

Based on the rheological and microstructural results, a schematic mechanism for the effect of ethanol on the gelation of  $\kappa$ -carrageenan gel was proposed (Fig. 8). It is generally considered that the gelation of  $\kappa$ -carrageenan solution involves two steps: the coil to double helix transition and the subsequent aggregation of the helices (Pedersen, 1980). When ethanol is introduced to  $\kappa$ -carrageenan aqueous solution, the strongly favourable hydration of ethanol in bulk aqueous phase might exclude water from the surrounding of  $\kappa$ -carrageenan molecules (Oakenfull, 2000), leading to reduced average amount of water molecules in the surrounding of  $\kappa$ -carrageenan molecules. The decreased water population deteriorates  $\kappa$ -carrageenan-water interactions, thereby making  $\kappa$ -carrageenan aggregate with their neighbourhood strands (Stenner, Matubayasi, & Shimizu, 2016). Additionally, cross-linking hydrogen bonds might be formed between the equatorial-OH groups of polyols and  $\kappa$ -carrageenan molecules (Ramakrishnan & Prud'homme, 2000), promoting the junction formation and aggregation. With increasing ethanol concentrations, more self-associations and coil-helix transitions of  $\kappa$ -carrageenan are expected to occur to form large junctions or aggregates, resulting in formation of denser and stronger gel networks.

#### 5. Conclusions

When  $\kappa$ -carrageenan solutions were added with ethanol, with increased amount of ethanol, the  $T_g$ ,  $T_m$ ,  $d_f$ ,  $S_g$  and  $G^*$  all increased while  $n$  decreased. All the  $\kappa$ -carrageenan gels formed strong gel networks demonstrating solid-like behaviour. The microstructure, as revealed by FESEM, of gels containing both 15 wt% and 20 wt% ethanol exhibited denser, finer, and compacter networks with less voids than  $\kappa$ -



carrageenan gel without ethanol or containing 5 wt% ethanol. Complementary to FESEM, SAXS analysis revealed that the average cross-sectional radii of  $\kappa$ -carrageenan strand increased upon ethanol addition. The rheology and microstructural results suggested that inclusion of ethanol up to 20 wt% facilitated  $\kappa$ -carrageenan gel formation and improved the gel strength by increasing the  $\kappa$ -carrageenan junction size and numbers.

Supplementary data to this article can be found online at <https://doi.org/10.1016/j.foodres.2018.03.016>.

## Conflict of interest

All the authors declare no conflict of interest.

## Acknowledgements

This work was funded by the Singapore NRF Industry-IHL Partnership Grant (R-143-000-653-281). The research was partly undertaken on the BL16B1 SAXS/WAXS beamline at the Shanghai Synchrotron, Shanghai, China. We thank F. Tian and P. Zhou from BL16B1 beamline at Shanghai Synchrotron Radiation Facility (SSRF) for assistance during SAXS data collection and processing.

## References

- Aramwit, P. (2016). Introduction to biomaterials for wound healing. In M. S. Agren (Vol. Ed.), *Wound healing biomaterials. Vol. 2. Wound healing biomaterials* (pp. 3–38). Duxford: Woodhead Publishing Inc.
- Beaucage, G. (1996). Small-angle scattering from polymeric mass fractals of arbitrary mass-fractal dimension. *Journal of Applied Crystallography*, 29(2), 134–146.
- Chambon, F., & Winter, H. H. (1985). Stopping of crosslinking reaction in a PDMS polymer at the gel point. *Polymer Bulletin*, 13(6), 499–503.
- Chambon, F., & Winter, H. H. (1987). Linear viscoelasticity at the gel point of a cross-linking PDMS with imbalanced stoichiometry. *Journal of Rheology*, 31(8), 683–697.
- Cuvelier, G., & Launay, B. (1990). Frequency dependence of viscoelastic properties of some physical gels near the gel point. *Macromolecular Symposia*, 40(1), 23–31.
- Denef, B., Mischenko, N., Koch, M. H. J., & Reynaers, H. (1996). Small-angle X-ray scattering of  $\kappa$ - and  $\lambda$ -carrageenan in aqueous and in salt solutions. *International Journal of Biological Macromolecules*, 18(3), 151–159.
- Gekko, K., Mugishima, H., & Koga, S. (1987). Effects of sugars and polyols on the sol-gel transition of  $\kappa$ -carrageenan: calorimetric study. *International Journal of Biological Macromolecules*, 9(3), 146–152.
- Hermansson, E., Schuster, E., Lindgren, L., Altskär, A., & Ström, A. (2016). Impact of solvent quality on the network strength and structure of alginate gels. *Carbohydrate Polymers*, 144, 289–296.
- Hilliou, L., Wilhelm, M., Yamanoi, M., & Gonçalves, M. P. (2009). Structural and mechanical characterization of  $\kappa/\lambda$ -hybrid carrageenan gels in potassium salt using Fourier transform rheology. *Food Hydrocolloids*, 23(8), 2322–2330.
- Hirun, N., Tantishaiyakul, V., Sangfai, T., Rugmai, S., & Soontaranon, S. (2016). Nanostructure, phase transition and morphology of gallic acid and xyloglucan hydrogel. *Polymer Bulletin*, 73(8), 2211–2226.
- Hollamby, M. J. (2013). Practical applications of small-angle neutron scattering. *Physical Chemistry Chemical Physics*, 15(26), 10566–10579.
- Hu, B., Lu, Y., Zhao, Q., & Matsukawa, S. (2017). A study on the gelation behavior of solutions of native gellan, deacylated gellan, and their mixture by water  $^1\text{H}$  T<sub>2</sub> measurements. *Food Hydrocolloids*, 72, 47–51.
- Joly-Duhamel, C., Heliou, D., Ajdari, A., & Djabourov, M. (2002). All gelatin networks: 2. The master curve for elasticity. *Langmuir*, 18(19), 7158–7166.
- Kavanagh, G. M., & Ross-Murphy, S. B. (1998). Rheological characterisation of polymer gels. *Progress in Polymer Science*, 23(3), 533–562.
- Lapasin, S. P. (1995). *Rheology of industrial polysaccharides: Theory and applications*. USA: Springer.
- Leiter, A., Mailänder, J., Wefers, D., Bunzel, M., & Gaukel, V. (2017). Influence of acid hydrolysis and dialysis of  $\kappa$ -carrageenan on its ice recrystallization inhibition activity. *Journal of Food Engineering*, 209, 26–35.
- Li, Z., Yang, Z., Otter, D., Rehm, C., Li, N., Zhou, P., & Hemar, Y. (2018). Rheological and structural properties of coagulated milks reconstituted in D<sub>2</sub>O: Comparison between rennet and a tamarillo enzyme (tamarillin). *Food Hydrocolloids*, 79, 170–178.
- Liu, S., Bao, H., & Li, L. (2016). Thermoreversible gelation and scaling laws for graphene oxide-filled  $\kappa$ -carrageenan hydrogels. *European Polymer Journal*, 79, 150–162.
- Liu, S., Huang, S., & Li, L. (2016). Thermoreversible gelation and viscoelasticity of  $\kappa$ -carrageenan hydrogels. *Journal of Rheology*, 60(2), 203–214.
- Liu, S., Li, H., Tang, B., Bi, S., & Li, L. (2016). Scaling law and microstructure of alginate hydrogel. *Carbohydrate Polymers*, 135, 101–109.
- Liu, S., & Li, L. (2016). Thermoreversible gelation and scaling behavior of Ca<sup>2+</sup>-induced  $\kappa$ -carrageenan hydrogels. *Food Hydrocolloids*, 61, 793–800.
- Lorén, N., Shtykova, L., Kidman, S., Jarvöll, P., Nydén, M., & Hermansson, A.-M. (2009). Dendrimer diffusion in  $\kappa$ -carrageenan gel structures. *Biomacromolecules*, 10(2), 275–284.
- Lu, L., Liu, X., Dai, L., & Tong, Z. (2005). Difference in concentration dependence of relaxation critical exponent n for alginate solutions at sol-gel transition induced by calcium cations. *Biomacromolecules*, 6(4), 2150–2156.
- Miyabe, Y., Furuta, T., Takeda, T., Kanno, G., Shimizu, T., Tanaka, Y., ... Kishimura, H. (2017). Structural properties of Phycoerythrin from *Dulse Palmaria palmata*. *Journal of Food Biochemistry*, 41(1), e12301.
- Muthukumar, M. (1989). Screening effect on viscoelasticity near the gel point. *Macromolecules*, 22(12), 4656–4658.
- Necas, J., & Bartosikova, L. (2013). Carrageenan: A review. *Veterinárni Medicína*, 58(4), 187–205.
- Nieto, T. V. N., Wang, Y., Ozimek, L., & Chen, L. (2016). Improved thermal gelation of oat protein with the formation of controlled phase-separated networks using dextrin and carrageenan polysaccharides. *Food Research International*, 82, 95–103.
- Oakenfull, D. (2000). Solvent structure and gelation of polysaccharides in concentrated solutions of simple sugars. In G. O. Phillips (Vol. Ed.), *Gums and Stabilisers for the Food Industry. Vol. 10. Gums and Stabilisers for the Food Industry* (pp. 277–284). Duxford: Woodhead Publishing Inc.
- Pedersen, J. K. (1980). Carrageenan, pectin and xanthan/locust bean gum gels. Trends in their food use. *Food Chemistry*, 6(1), 77–88.
- Ramakrishnan, S., & Prud'homme, R. K. (2000). Behavior of  $\kappa$ -carrageenan in glycerol and sorbitol solutions. *Carbohydrate Polymers*, 43(4), 327–332.
- Rhim, J.-W. (2013). Effect of PLA lamination on performance characteristics of agar/ $\kappa$ -carrageenan/clay bio-nanocomposite film. *Food Research International*, 51(2), 714–722.
- Robal, M., Brenner, T., Matsukawa, S., Ogawa, H., Truus, K., Rudolph, B., & Tuvikene, R. (2017). Monocationic salts of carrageenans: Preparation and physico-chemical properties. *Food Hydrocolloids*, 63, 656–667.
- Schuster, E., Cucheval, A., Lundin, L., & Williams, M. A. K. (2011). Using SAXS to reveal the degree of bundling in the polysaccharide junction zones of microrheologically distinct pectin gels. *Biomacromolecules*, 12(7), 2583–2590.
- Şen, M., & Erboz, E. N. (2010). Determination of critical gelation conditions of  $\kappa$ -carrageenan by viscosimetric and FT-IR analyses. *Food Research International*, 43(5), 1361–1364.
- Sow, L. C., Kong, K., & Yang, H. (2018). Structural modification of fish gelatin by the addition of gellan,  $\kappa$ -carrageenan, and salts mimics the critical physicochemical properties of pork gelatin. *Journal of Food Science*. <http://dx.doi.org/10.1111/1750-3841.14123>.
- Stenner, R., Matubayasi, N., & Shimizu, S. (2016). Gelation of carrageenan: Effects of sugars and polyols. *Food Hydrocolloids*, 54(Part B), 284–292.
- Stokke, B. T., Draget, K. I., Smidsrød, O., Yuguchi, Y., Urakawa, H., & Kajiwara, K. (2000). Small-angle X-ray scattering and rheological characterization of alginate gels. 1. Ca-alginate gels. *Macromolecules*, 33(5), 1853–1863.
- Tari, Ö., Kara, S., & Pekcan, Ö. (2009). Critical exponents of kappa carrageenan in the coil-helix and helix-coil hysteresis loops. *Journal of Macromolecular Science, Part B: Physics*, 48(4), 812–822.
- Teodorescu, M., Morariu, S., Bercea, M., & Sacarescu, L. (2016). Viscoelastic and structural properties of poly(vinyl alcohol)/poly(vinylpyrrolidone) hydrogels. *RSC Advances*, 6(46), 39718–39727.
- Tho, I., Kjøniksen, A.-L., Knudsen, K. D., & Nyström, B. (2006). Effect of solvent composition on the association behavior of pectin in methanol–water mixtures. *European Polymer Journal*, 42(5), 1164–1172.
- Tho, I., Kjøniksen, A.-L., Nyström, B., & Roots, J. (2003). Characterization of association and gelation of pectin in methanol-water mixtures. *Biomacromolecules*, 4(6), 1623–1629.
- Wang, Y., & Padua, G. W. (2010). Formation of zein microphases in ethanol-water. *Langmuir*, 26(15), 12897–12901.
- Wu, Y., Cui, W., Eskin, N. A. M., & Goff, H. D. (2009). Rheological investigation of synergistic interactions between galactomannans and non-pectic polysaccharide fraction from water soluble yellow mustard mucilage. *Carbohydrate Polymers*, 78(1), 112–116.
- Xu, W., Jin, W., Zhang, C., Li, Z., Lin, L., Huang, Q., ... Li, B. (2014). Curcumin loaded and protective system based on complex of  $\kappa$ -carrageenan and lysozyme. *Food Research International*, 59, 61–66.
- Yang, B., Yu, G., Zhao, X., Ren, W., Jiao, G., Fang, L., ... Zhang, J. (2011). Structural characterisation and bioactivities of hybrid carrageenan-like sulphated galactan from red alga *Furcellaria lumbicalis*. *Food Chemistry*, 124(1), 50–57.
- Yang, Z., Chaieb, S., Hemar, Y., de Campo, L., Rehm, C., & McGillivray, D. J. (2015). Investigating linear and nonlinear viscoelastic behaviour and microstructures of gelatin-multiwalled carbon nanotube composites. *RSC Advances*, 5(1300), 107916–107926.
- Yang, Z., Hemar, Y., Hilliou, L., Gilbert, E. P., McGillivray, D. J., Williams, M. A. K., & Chaieb, S. (2016). Nonlinear behavior of gelatin networks reveals a hierarchical structure. *Biomacromolecules*, 17(2), 590–600.
- Yang, Z., Yang, H., & Yang, H. (2018). Effects of sucrose addition on the rheology and microstructure of  $\kappa$ -carrageenan gel. *Food Hydrocolloids*, 75, 164–173.
- Zhang, T., Xu, X., Ji, L., Li, Z., Wang, Y., Xue, Y., & Xue, C. (2017). Phase behaviors involved in surimi gel system: Effects of phase separation on gelation of myofibrillar protein and kappa-carrageenan. *Food Research International*, 100(part 1), 361–368.
- Zhu, J.-H., Yang, X.-Q., Ahmad, I., Li, L., Wang, X.-Y., & Liu, C. (2008). Rheological properties of  $\kappa$ -carrageenan and soybean glycinin mixed gels. *Food Research International*, 41(3), 219–228.